Journal of Materials Chemistry C

PAPER

View Article Online
View Journal | View Issue



Cite this: J. Mater. Chem. C, 2014, 2, 4415

# A thin all-elastomeric capacitive pressure sensor array based on micro-contact printed elastic conductors†

Su-Jeong Woo,[a] Jeong-Ho Kong,[a] Dae-Gon Kim[b] and Jong-Man Kim*[ab]

Received 27th February 2014
Accepted 25th March 2014

DOI: 10.1039/c4tc00392f

www.rsc.org/MaterialsC

We present a highly elastic capacitive pressure sensor array based on a thin all-elastomeric platform suitable for being integrated onto surfaces with a complex curvature like human skin. The proposed skin-like sensors are simply fabricated by a combination of soft-lithographic replication and contact printing based micro-patterning of a conductive elastomeric ink (carbon nanotube (CNT)-doped polydimethylsiloxane (PDMS)) in a precise and cost-effective manner. The electrical responses of the devices are highly linear, reliable, and reversible when subjected to pressure and tensile strain. Moreover, the devices are mechanically robust enough to be operated stably under various elastic deformations without any structural failure or degradation in performance. In addition, we show that the sensors have possibilities for being employed practically as artificial skins by demonstrating devices that can detect different types of human motions (finger bending and gripping) and spatial pressure distributions generated by the stamps with different protrusion patterns.

## Introduction

Recently, pressure-sensitive artificial skins have received significant attention for their potential applications in skin-like wearable electronics, prosthetics, and robotics. Pressure sensor arrays that can measure the external force in response to physical contact with objects are essential components to recognize tactile information in these applications. Advances in semiconductors and microelectromechanical systems (MEMS) make it possible to realize highly sensitive and compact-sized tactile sensors in the form of an array of pressure sensors based on versatile silicon-micromachining techniques.[1–5] However, silicon-based tactile sensors have two critical limitations in their practical applications as artificial skins. First, the sensor structures with tiny silicon parts, such as bridges and membranes, are not suitable for sustaining large deformation and abrupt impacts because of the brittle nature of the silicon material. In addition, it is infeasible for the silicon-based sensors to be implemented on curved surfaces because they are based mainly on a rigid silicon platform. To overcome these limitations, various geometries of tactile sensors have been demonstrated in mechanically flexible platforms based on plastic or elastomeric substrates such as polyimide (PI), polycarbonate (PC), polyethylene terephthalate (PET), polyethylene naphthalate (PEN), and polydimethylsiloxane (PDMS).[6–22] In general, two sensing principles, resistive and capacitive, have been frequently employed for providing tactile information by recognizing changes in electrical resistance and capacitance in response to external pressure in flexible sensors. In resistive techniques, piezoresistors have often been incorporated with flexible platforms,[6–12] and pressure-sensitive rubber sheets or disks have been used as tactile sensing materials integrated with a flexible sensor circuitry.[13–19] In capacitive approaches, capacitor arrays consisting mainly of parallel-plate coupling electrode pairs incorporated with flexible substrates have been most widely used to recognize the tactile input.[20–22] Compared to the silicon-based approaches, these flexible tactile sensors can be easily applied to simple curved surfaces, like cylindrical objects, without significant degradation in performance. However, they would be inadequate for application to more complex three-dimensional surfaces, because the metallic and metal-oxide thin-films used usually as piezoresistors, electrodes, and interconnects in such systems are highly susceptible to possible failures related to cracks, fractures, and fatigue under both large stretching to cover complex surfaces and repetitive operations. Recently, several alternatives have been proposed to overcome the limitations of conventional flexible tactile sensors by demonstrating artificial skin-like sensors that can cover complex surfaces conformally and are robust against mechanical failure.[23–27] M.-Y. Cheng *et al.* proposed a highly twistable tactile sensing array using conductive polymer sensing materials and stretchable helical electrodes based on a

[a]Department of Nano Fusion Technology, Pusan National University, Busan 609-735, Republic of Korea. E-mail: jongkim@pusan.ac.kr

[b]Department of Nanomechatronics Engineering, Pusan National University, Busan 609-735, Republic of Korea

† Electronic supplementary information (ESI) available: Ecoflex thickness as a function of spin speed; capacitance change ratio of the device due to various force-loading speeds. See DOI: 10.1039/c4tc00392f

PDMS platform.[23] M. Shimojo *et al.* reported a tactile sensor sheet based on pressure-sensitive rubber stitched with electrical wires.[24] Although the developed sensing arrays are suitable for covering complex surfaces without severe damage on the structures, the fabrication is quite cumbersome and complex, resulting in incompatibility with mass-production. R. D. P. Wong *et al.* reported a relatively new class of capacitive normal force sensors based on liquid metal-filled microfluidic channels.[25] However, there is a possible leakage problem of the conductive fluids from the assembled PDMS channels under repetitive pressurized conditions, resulting in instability in long-term use. D. J. Lipomi *et al.* developed a skin-like pressure sensor array capable of conformal contact on complex surfaces based on elastic electrodes of carbon nanotubes (CNTs) prepared by a simple spray-coating method.[26] However, the percolated CNT electrodes are formed only on top of the elastic substrate, which makes it possible for them to delaminate under repetitive sensor operations. S. Yao *et al.* reported wearable capacitive sensors based on highly elastic conductors made of silver nanowires (AgNWs).[27] Mechanical robustness of the sensor architectures can be improved by embedding the patterned AgNW conductors into a PDMS matrix using a shadow mask approach.[28] However, the shadow mask-based patterning method may suffer from relatively low accuracy and reproducibility. More recently, M. Kaltenbrunner *et al.* demonstrated a pioneering study dealing with an ultraflexible tactile sensing sheet consisting of resistive tactile sensor pixels and field effect transistors (FETs) on ultrathin plastic foil.[29] Although the imperceptible sensing foils can fit arbitrary dynamic surfaces excellently by forming intimate contact, it is challenging to maintain their performance under large deformation circumstances because they still include metallic components such as electrodes and interconnects.

Here, we present an all-elastomeric skin-like pressure sensor array consisting of conductive PDMS (CPDMS, electrodes, and interconnects)[30,31] and insulative elastomeric (plates and dielectrics) architectures. The thin all-elastomeric platform can ensure mechanical robustness against various elastic deformations and exfoliation, and conformal covering capability to complex surfaces without imposing mechanical constraints while retaining linear, reliable, and reversible electrical performance. Another important advantage of the proposed approach is the simple and cost-effective fabrication based on facile soft-lithographic replication and micro-contact printing (μCP) techniques of the CPDMS ink.

# Experimental section

### Synthesis of CPDMS ink

CPDMS ink is a key material for fabricating the elastic conductors used as both electrodes and interconnects in the proposed skin-like pressure sensor array. The ink was prepared simply by dispersing conductive nanofillers in a PDMS matrix. CNTs (10 wt% with respect to the PDMS prepolymer) were employed as conductive filler materials to produce the elastic conductors, because CNT-based electrical networks incorporated with elastomeric materials are more favorable for retaining electrical performance under elastic deformations such as bending and stretching due to the high aspect ratio of the CNTs.[32] In detail, the multi-walled CNTs were first blended in a volatile solvent (toluene) at a weight ratio of 1 : 6, and the CNT/toluene suspension was then stirred magnetically to make it easy for the CNTs to disperse well in the solvent. After stirring for 2 h, the suspension was mixed with liquid PDMS (Sylgard 184 A, Dow Corning), which was diluted with toluene (a weight ratio of 1 : 1). The liquid mixture (CNT–PDMS–toluene) was further stirred magnetically on a hotplate (set at 70 °C) to entirely evaporate the solvent components from the mixture, which can greatly help in preparing CPDMS ink with uniform electrical properties.

### Sensor architecture and fabrication

Fig. 1 presents a schematic illustration of the proposed skin-like sensor based on a thin all-elastomeric platform. This platform makes it possible for the device to be operated stably without any mechanical failure even under extreme and repetitive operational conditions when mounted on human skin. The sensor consists of 16 individual capacitively coupled pressure sensing cells to detect the external tactile information in a $4 \times 4$ arrayed configuration, and each capacitive pressure-sensing cell is composed of a pair of CPDMS sensing electrodes facing each other across the elastomeric insulating layer to construct a parallel-plate capacitor. The CPDMS sensing electrodes are biased electrically through CPDMS wires bridging the sensing and probing electrodes. An Ecoflex silicone elastomer capable of being more easily deformed than PDMS was utilized as the intermediate insulating layer. In principle, the capacitance of the pressure sensor can be changed relying on the change in the inter-electrode gap distance induced by the applied pressure as shown in Fig. 1. In proportion to the applied normal force, the upper and lower CPDMS sensing electrodes become closer to each other, resulting in an increase of the capacitance, and *vice versa*.

The proposed skin-like sensors were fabricated by facile soft-lithographic replication and CPDMS ink-based μCP techniques. Key fabrication steps for the sensors are illustrated schematically in Fig. 2. A ~80 μm thick photoresist (PR, JSR THB-151N) micro-mold was first formed on a 4-inch silicon substrate by a standard photolithography process to prepare the PDMS stamps employed as the parallel-plates of a capacitor after printing the CPDMS ink (Fig. 2a). The PDMS prepolymer was mixed with a curing agent (Sylgard 184 B, Dow Corning) at a weight ratio of 10 : 1 and cast on the prepared PR molds by spin-coating at 300 rpm. Subsequently, PDMS was fully cured at 70 °C for 30 min after degassing to entirely remove the air-bubbles trapped in the liquid PDMS using a vacuum desiccator. After peeling off the solidified PDMS from the mold substrate, the PDMS stamps were ready for accepting the CPDMS ink (Fig. 2b). The synthesized CPDMS ink was mixed with the curing agent at a weight ratio of 10 : 3 and cast onto another silicon substrate uniformly using a rubber blade. The CPDMS conductors were then patterned in a precise manner by transferring the CPDMS ink onto the protruding parts of the PDMS stamp using a

 

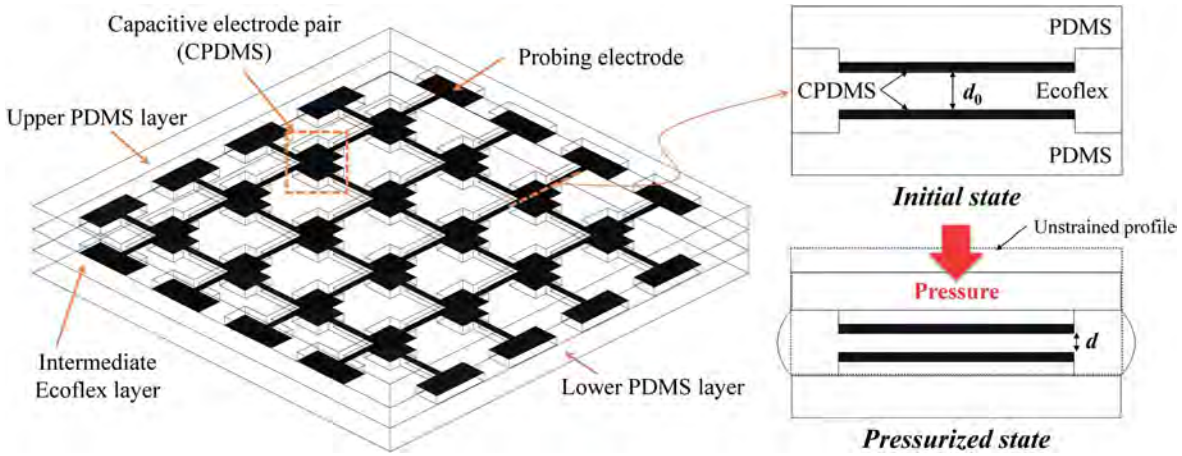


Fig. 1 Schematic illustration of the proposed all-elastomeric skin-like pressure sensor array.

manual *xyz*-stage under slight pressure, and the patterned CPDMS ink was thermally cured at 70 °C for 1 h (Fig. 2c). It is noteworthy that the μCP technique makes the fabrication of the sensor simple by enabling the preparation of CPDMS conductors including sensing/probing electrodes and interconnects through one-time contact printing. After electrically wiring to the probing electrodes for each address line using a silver paste (not shown for convenience), the insulating layer was deposited onto the CPDMS-printed side of the PDMS stamp. For this, the Ecoflex base polymer (0010, Smooth-on) mixed with a cross-linker at a weight ratio of 1 : 1 was first spin-coated at 500 rpm. The thickness of the intermediate Ecoflex layer can be easily controlled by changing the spin speed as shown in Fig. S1.† In succession, the substrate was maintained at room temperature for 3 h to flatten the Ecoflex layer coated onto the uneven stamp surface while curing slightly (Fig. 2d). The planarization and semi-curing of the Ecoflex layer are crucial for both conformal contact and reliable bonding between two CPDMS plates by making the surfaces of each plate flat and sticky in the following assembly step. In addition, semi-curing is also greatly helpful for obtaining an exact thickness of the intermediate layer by preventing the Ecoflex from flowing out in between the two plates during pressurization, resulting in predictable electrical performance. A second CPDMS plate (a counterpart to the first plate to form a parallel-plate capacitor) prepared by the same fabrication procedures (Fig. 2a–d) was oriented perpendicular to the first plate and assembled after careful alignment (Fig. 2e). Finally, the assembled plates were thermally cured at 80 °C for

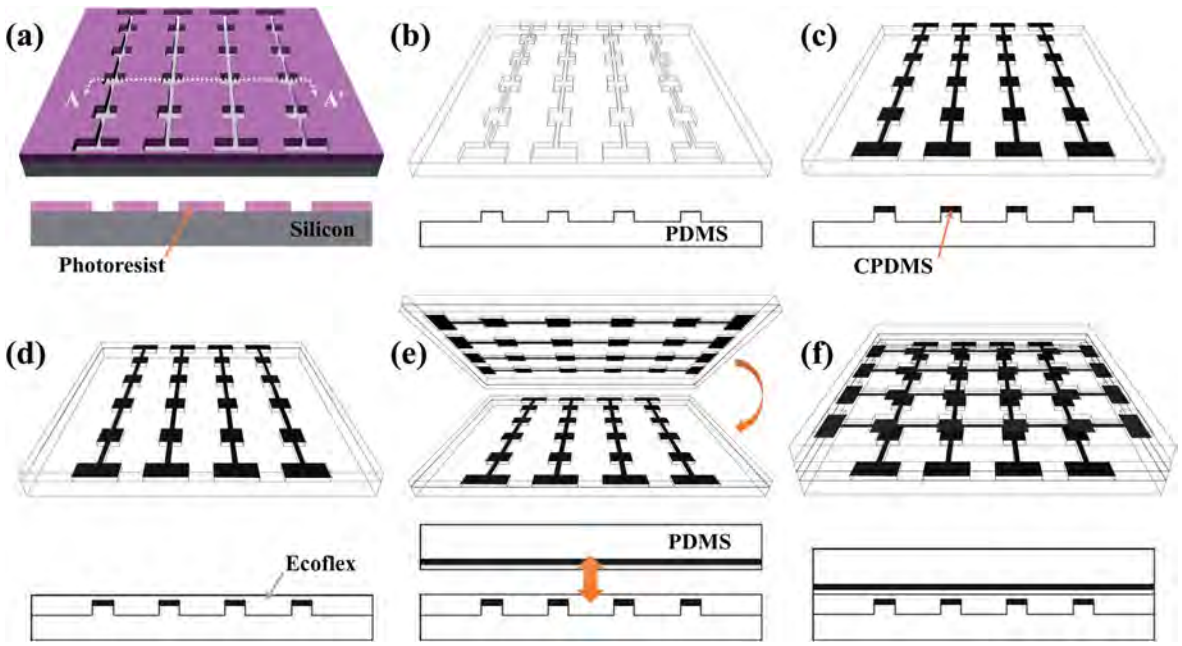


Fig. 2 Schematic illustrations of fabrication procedures for the skin-like pressure sensor array. (a) PR micro-mold formation (photolithography), (b) PDMS stamp replication, (c) CPDMS patterning (micro-contact printing), (d) intermediate Ecoflex layer spin-coating, (e) alignment and assembly, and (f) final thermal curing.

1 h with the application of pressure for complete contact between the two plates (Fig. 2f).

### Evaluation of sensor performance

To evaluate the response characteristics of the skin-like sensors under elastic deformations, the fabricated device was mounted on a motorized stand (JSV-H1000, JISC) equipped with a push–pull force gauge (H-10, JISC), and its electrical properties (resistance and capacitance) were measured and recorded in real time using an LCR meter (Model-6375, Microtest) interfaced to a computer with a data cable (RS-232). A normal force was applied to the device by using a flat-top cylindrical tip with a radius of ~2.25 mm connected to the push–pull force gauge with a loading speed of 1 mm $min^{-1}$. Tensile strain was applied to the unit sensing cell using the computer-controlled motorized system with a loading speed of 1 mm $min^{-1}$. For electrical measurements, electrical wires were connected to probing electrodes of the device using a silver paste. A two-probe method was employed to measure the change in the electrical resistance due to variations in the printing number using a probe station (MST-4000A, MS TECH).

## Results and discussion

Fig. 3 shows the patterning results and fabricated device based on the proposed μCP technique. The CPDMS conductors were patterned precisely on the PDMS stamp by the μCP technique as shown in Fig. 3a. It should be noted that the electrical properties of the CPDMS conductors can be enhanced by increasing the number of printings. The electrical resistance was exponentially decreased with the increased number of printings by up to five times as shown in Fig. 3b. This suggests that the resultant thickness is quite uniform for each printing time because the change in resistance predominantly depends on the change in thickness of the printed CPDMS pattern with respect to the fixed length. Fig. 3c shows the fabrication-completed skin-like sensor with a cross-sectional optical image (the inset in Fig. 3c), which indicates that all the parts of the sensor were well-structured as a film (~1 mm in thickness) by the described fabrication approach. The mechanical robustness of the fabricated sensor was also clearly demonstrated under various elastic deformations like bending, stretching, twisting, and folding, as shown in Fig. 3d.

The electrical performance of the CPDMS conductor was first characterized by applying a normal force (a loading speed of 1 mm $min^{-1}$) to the unit sensing cell. With the applied pressure, the CPDMS conductor is deformed maximally at the parts forced by the edges of a loading object, resulting in an increase in the electrical resistance of the conductor. Nevertheless, the change in resistance of the CPDMS conductor was not significant under a loading pressure of up to ~1.2 MPa, which corresponds to ~20 N in force, as shown in Fig. 4a. This

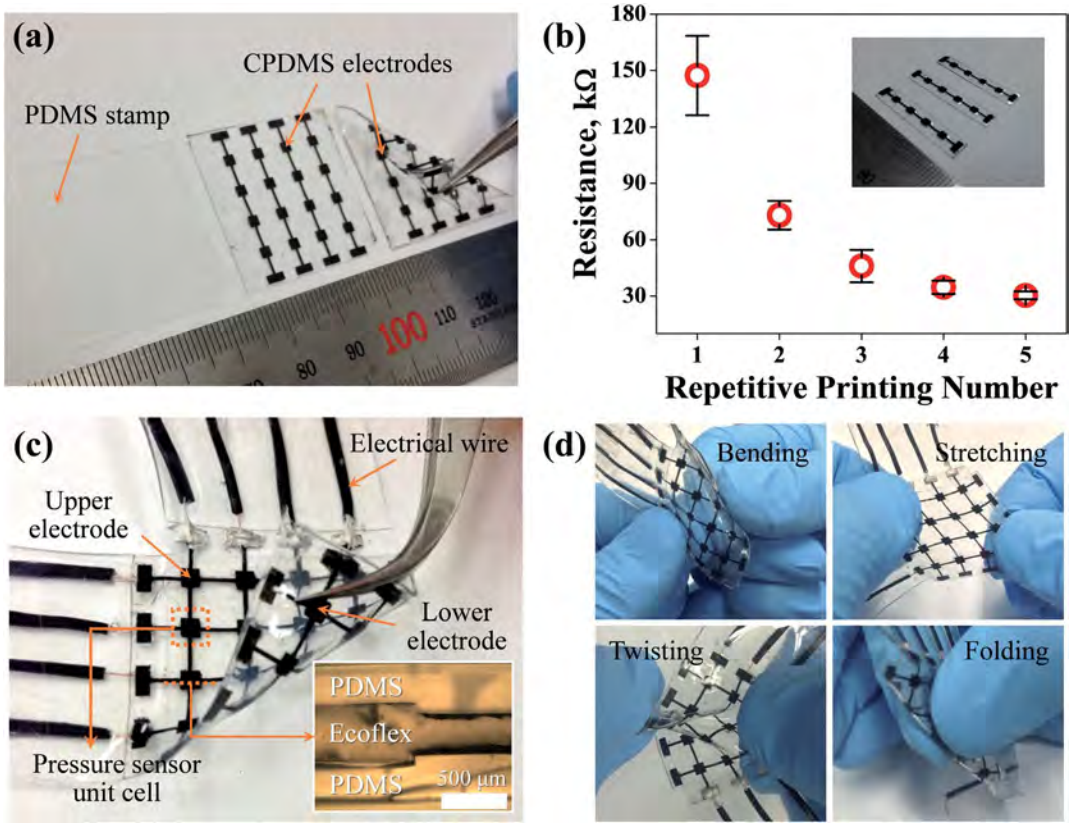


Fig. 3 Fabrication results. (a) CPDMS conductors prepared by the μCP technique (electrode size: 2 × 2 $mm^2$, center-to-center inter-electrode spacing: 6 mm), (b) electrical resistance due to the printing number, (c) fabrication-completed skin-like sensor (inset: cross-sectional digital image), and (d) fabricated sensor under various deformations.

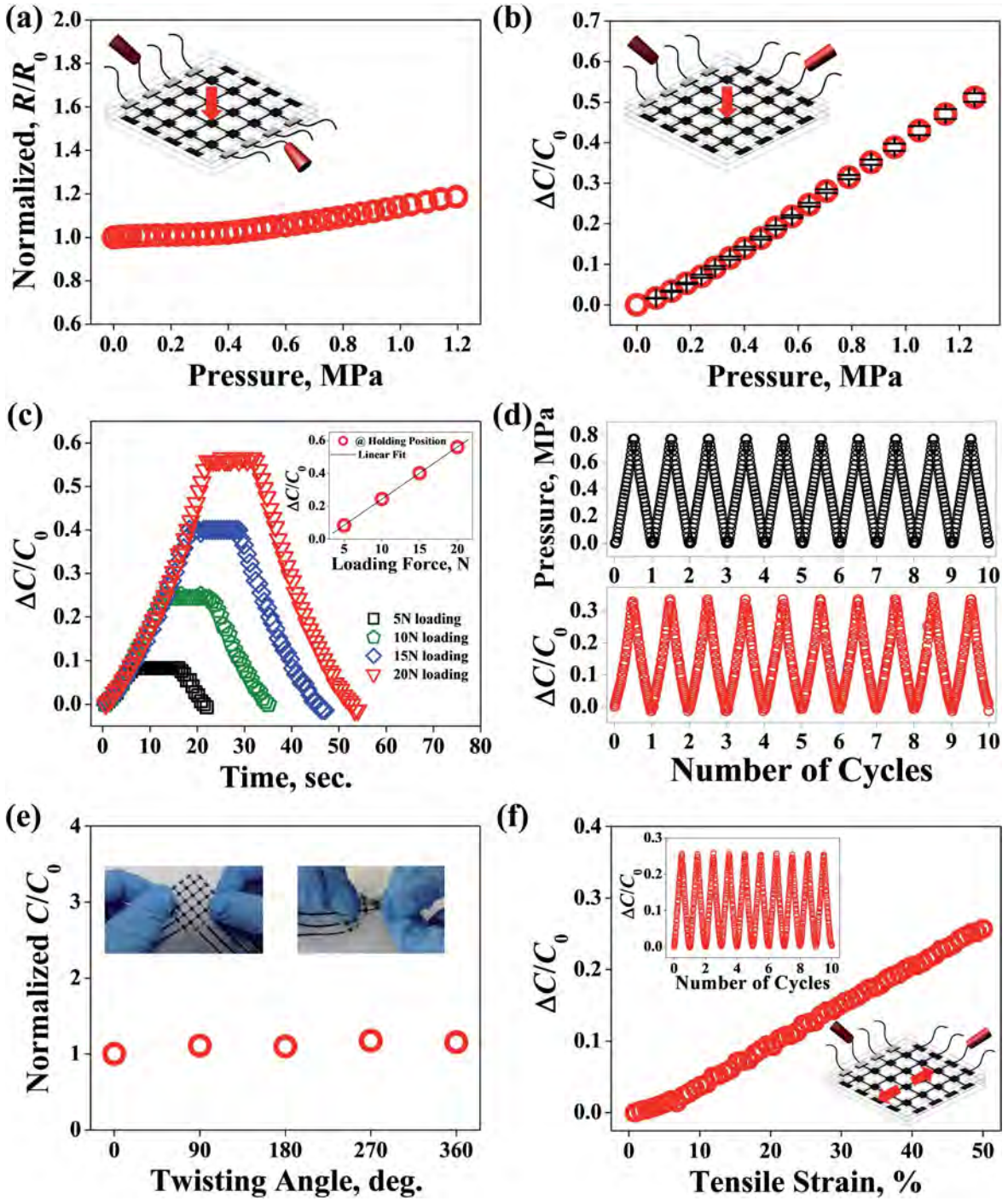


Fig. 4 Performance evaluations of the fabricated skin-like sensor. (a) Normalized electrical resistance of the CPDMS conductor under an applied pressure of up to ~1.2 MPa, (b) capacitance change ratio ($\Delta C/C_0$) under an applied pressure of up to ~1.2 MPa, (c) $\Delta C/C_0$ due to sequential operations with various loading forces (inset: $\Delta C/C_0$ in each holding state), (d) $\Delta C/C_0$ under repetitive loading/unloading cycles with a maximum pressure of up to ~0.8 MPa, (e) normalized capacitance under progressively increasing twisting deformations with an applied pressure of up to ~0.8 MPa, and (f) $\Delta C/C_0$ under an applied tensile strain of up to 50% (inset: $\Delta C/C_0$ under repetitive stretching/releasing cycles).

evidences that the percolated CNT networks in the CPDMS conductor can fairly withstand the applied pressure without a remarkable loss of current paths. Fig. 4b shows the capacitance change ratio ($\Delta C/C_0$) depending on the applied pressure. The capacitance was increased in a linear manner with respect to the applied pressure of up to ~1.2 MPa indicating a minimum detectable pressure of less than 50 kPa. In addition, the capacitive responses of the sensor were also found to be highly reliable and reversible. Fig. 4c shows the change in capacitance due to sequential operations (force loading at 1 mm $min^{-1}$ → holding for 10 s → force unloading at 1 mm $min^{-1}$) of the device under various loading forces. The capacitance values in

holding states for each loading force were retained perfectly with little deviation and also maintained a linear relationship with the loading force (the inset in Fig. 4c). In addition, the holding capacitances were returned to their initial values when the applied forces were removed entirely, showing a similar slope. Moreover, the slope in the capacitance change can be tailored easily by changing the force loading speed, as shown in Fig. S2.† The device was also operated stably ensuring both reliability and reversibility even under continuous force loading/unloading cycles as shown in Fig. 4d. The mechanical robustness of the device was evaluated simply by a twisting test for a sensing cell. With the application of progressively increasing twisting deformations (initial → 90° → rest → 180° → rest → 270° → rest → 360° → rest), the capacitance change ratios at each rest state of the sensing cell were measured under the applied pressure of ~0.8 MPa and normalized with the initial ratio as shown in Fig. 4e. In this case, $C_0$ is defined as the capacitance measured under the pressure of ~0.8 MPa at the initial state of the sensing cell. The capacitance change ratios were maintained at similar values without large deviation with respect to the initial ratio. This indicates that no irrecoverable structural distortion occurred in the sensor platform, even after undergoing severe twisting deformations, thanks to its all-elastomeric configuration. The proposed skin-like sensor can also react stably with tensile strain. Fig. 4f shows the capacitive responses for the device when subjected to a tensile strain ($\varepsilon$) of up to 50%. The capacitance change was linearly proportional to the applied tensile strain maintaining a near-constant gauge factor of ~0.55, which is defined as $(\Delta C/C_0)/\varepsilon$. The device was also found to be reliable and reversible in cyclic stretching and releasing operations (the inset in Fig. 4f).

To show the practical usability of the proposed skin-like sensor, several tests were carried out with the device being worn on a human finger with the help of its flexible nature. We first detected the finger motions by monitoring the change in capacitance of a sensing cell as a function of time due to the degree of finger bending as shown in Fig. 5a. When the finger integrated with the fabricated sensor, which was aligned to a finger joint, was bent slightly, the capacitance of the sensing cell was increased moderately (region (II)), and it was recovered stably close to its initial value (region (I)) upon straightening. In addition, further bending of the finger led to a larger increase in capacitance and successive bending/straightening finger motions were distinguishable (region (III)). Another practical test was performed while keeping a tight grip on an object (a quail egg) by the finger integrated with the device as shown in Fig. 5b. When the gripping force was increased, the capacitance of the sensing cell facing the egg was accordingly increased. It is noteworthy that similar levels of the applied forces during repetitive loading/unloading cycles induced similar values of the resultant capacitances (region (II)). The change in capacitance became the greatest just before the egg was cracked (region (III)), and the maximized capacitance subsequently came back to its starting value (region (V), similar to region (I)) after experiencing a short transient state (slight fluctuations in capacitance, region (IV)) when the egg was fully broken.

Finally, the fabricated skin-like sensor with the 16 individual pressure-detecting cells was tested as a sensor for detecting spatial tactile information. Before the test, the capacitances of each sensing cell were measured under initial and pressurized conditions as shown in Fig. 6a and b. The initial capacitance of the sensing cells was measured to be 2.66 ± 0.28 pF in the initial state and the average capacitance of each cell was increased to 3.18 pF with a relatively small standard deviation of 0.36 pF in response to an applied pressure of ~0.5 MPa. As a result, the corresponding average $\Delta C/C_0$ of each cell was characterized to be 0.2 ± 0.02 (Fig. 6c). This reflects that the capacitive responses of the device were quite uniform and stable. Fig. 6d shows the

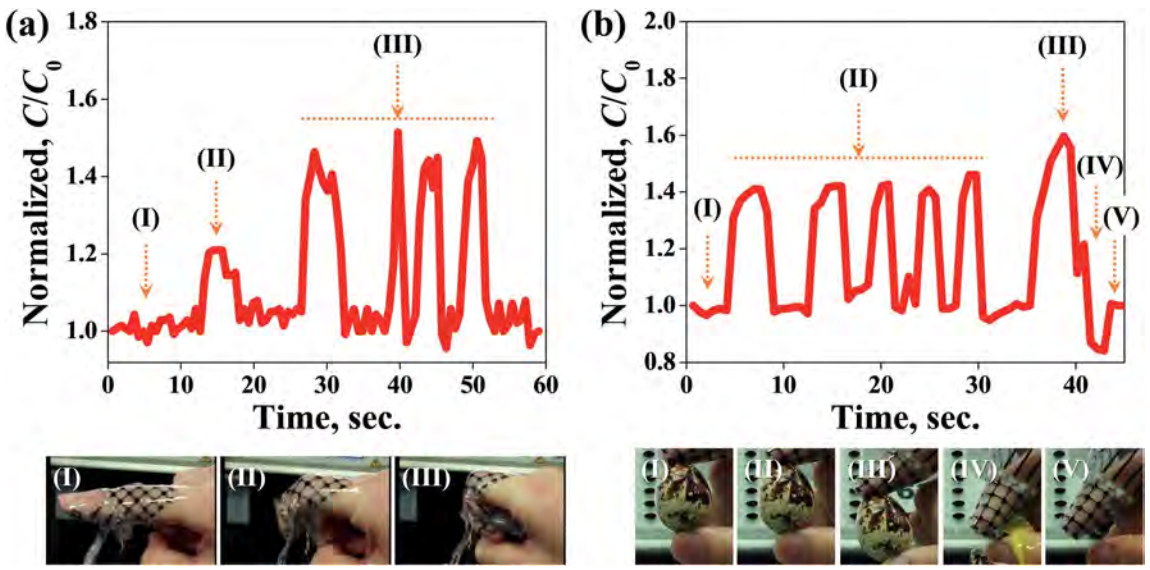


Fig. 5 Applications of the fabricated pressure sensor array integrated on the human finger as a skin-like sensor. (a) Normalized capacitance with finger bending motions, and (b) normalized capacitance under various gripping forces with a quail egg.

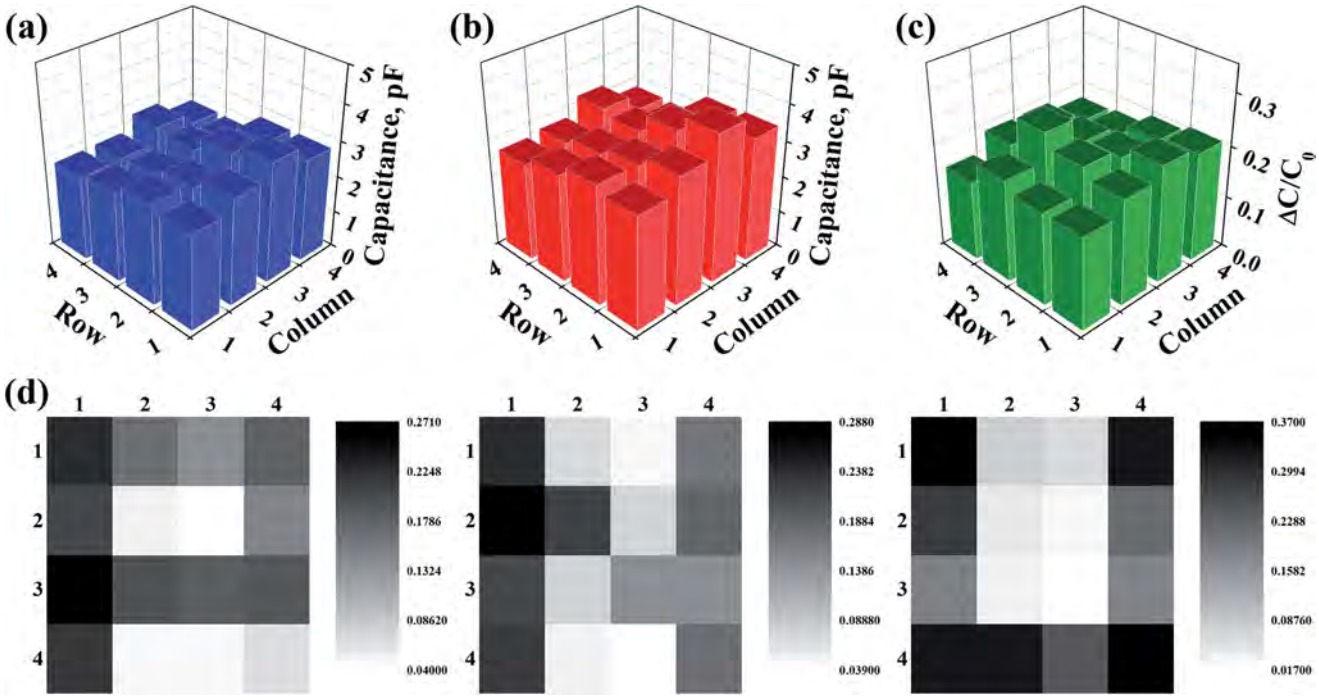


Fig. 6 Capacitance distributions measured on the fabricated pressure sensor array. (a) Initial capacitance distributions (2.66 ± 0.28 pF), (b) capacitance distributions under an applied pressure of ~0.5 MPa (3.18 ± 0.36 pF), (c) $\Delta C/C_0$ of each cell (0.2 ± 0.02), and (d) capacitance distributions using stamps with different patterns (the initials of our institution: 'P', 'N' and 'U').

capacitance distributions measured on the 4 × 4 pressure sensor array while applying pressure by stamps with different patterns (the initials of our institution: 'P', 'N' and 'U'). The different patterns on stamps were successfully transferred to the corresponding image plots, which could clearly be recognized as distinguishable characters, with a fairly low crosstalk between each adjacent sensing cell, as shown in Fig. 6d. These experimental observations clearly suggest that the proposed skin-like sensor is practically applicable to artificial skin owing to its robustness in terms of mechanical and electrical performance.

## Conclusions

In summary, we have demonstrated an artificial skin with a pressure sensor array based on a thin all-elastomeric platform (~1 mm in thickness), which is highly suitable for being integrated onto human skin, with several advantages in terms of the electrical and mechanical performance. The proposed devices were easily fabricated by a simple combination of the well-established soft-lithography and scalable CPDMS-based μCP techniques. The fabricated sensors were mechanically robust against stretching, bending, twisting, and folding deformations without any mechanical failures in the sensor structures, such as cracks, fractures, and exfoliation of the elastic conductors, thanks to their all-elastomeric architectures. The electrical responses of the devices were highly linear, reliable and reversible under repetitive applications of pressure and tensile strain, and showed little dependence on severe mechanical deformations (twisting up to 360°). In addition, the capacitive responses of each sensing cell consisting of the proposed skin-like sensor were considerably uniform with relatively small standard deviations in both initial and deformed states, which is highly desirable for detecting spatial tactile information. In addition, several practical tests demonstrated that the fabricated devices are greatly feasible for being employed as artificial skins in practical applications. Based on the desirable features of the proposed all-elastomeric sensor platforms including mechanical robustness, electrical reliability and simple, cost-effective fabrication, the devices will have potential applications in skin-like wearable and stretchable electronics.

## Acknowledgements

This work was supported by a 2-Year Research Grant of Pusan National University.

## Notes and references

1 M. R. Wolffenbuttel and P. P. L. Regtien, *Sens. Actuators, A*, 1990, **24**, 187.
2 B. J. Kane, M. R. Cutkosky and G. T. A. Kovacs, *J. Microelectromech. Syst.*, 2000, **9**, 425.
3 M. Ádám, T. Mohácsy, P. Jónás, C. Dücső, É. Vázsonyi and I. Bársony, *Sens. Actuators, A*, 2008, **142**, 192.
4 H. B. Muhammad, C. Recchiuto, C. M. Oddo, L. Beccai, C. J. Anthony, M. J. Adams, M. C. Carrozza and M. C. L. Ward, *Microelectron. Eng.*, 2011, **88**, 1811.

5 H. B. Muhammad, C. M. Oddo, L. Beccai, C. Recchiuto, C. J. Anthony, M. J. Adams, M. C. Carrozza, D. W. L. Hukins and M. C. L. Ward, *Sens. Actuators, A*, 2011, **165**, 221.
6 E.-S. Hwang, J.-H. Seo and Y.-J. Kim, *J. Microelectromech. Syst.*, 2007, **16**, 556.
7 H.-J. Kwon and W.-C. Choi, *Microsyst. Technol.*, 2010, **16**, 2029.
8 J. Engel, J. Chen and C. Liu, *J. Micromech. Microeng.*, 2003, **13**, 359.
9 R. Kilaru, Z. Ç. Butler, D. P. Butler and I. E. Gönenli, *J. Microelectromech. Syst.*, 2013, **22**, 349.
10 S.-H. Kim, J. Engel, C. Liu and D. L. Jones, *J. Micromech. Microeng.*, 2005, **15**, 912.
11 Y.-J. Yang, M.-Y. Cheng, S.-C. Shih, X.-H. Huang, C.-M. Tsao, F.-Y. Chang and K.-C. Fan, *Int. J. Adv. Des. Manuf. Technol.*, 2010, **46**, 945.
12 Y. Zhang, *J. Micromech. Microeng.*, 2010, **20**, 085012.
13 M.-Y. Cheng, X.-H. Huang, C.-W. Ma and Y.-J. Yang, *J. Micromech. Microeng.*, 2009, **19**, 115001.
14 H.-K. Kim, S. Lee and K.-S. Yun, *Sens. Actuators, A*, 2011, **165**, 2.
15 H. Z. Zhang, Q. Y. Tang and Y. C. Chan, *AIP Adv.*, 2012, **2**, 022112.
16 S. C. B. Mannsfeld, B. C.-K. Tee, R. M. Stoltenberg, C. V. H.-H. Chen, S. Barman, B. V. O. Muir, A. N. Sokolov, C. Reese and Z. Bao, *Nat. Mater.*, 2010, **9**, 859.
17 H.-K. Lee, S.-I. Chang and E. Yoon, *J. Microelectromech. Syst.*, 2006, **15**, 1681.
18 H.-K. Lee, J. Chung, S.-I. Chang and E. Yoon, *J. Microelectromech. Syst.*, 2008, **17**, 934.
19 P. Peng, R. Rajamani and A. G. Erdman, *J. Microelectromech. Syst.*, 2009, **18**, 1226.
20 T. Someya, T. Sekitani, S. Iba, Y. Kato, H. Kawaguchi and T. Sakurai, *Proc. Natl. Acad. Sci. U. S. A.*, 2004, **101**, 9966.
21 T. Sekitani, T. Yokota, U. Zschieschang, H. Klauk, S. Bauer, K. Takeuchi, M. Takamiya, T. Sakurai and T. Someya, *Science*, 2009, **326**, 1516.
22 K. Takei, T. Takahashi, J. C. Ho, H. Ko, A. G. Gillies, P. W. Leu, R. S. Fearing and A. Javey, *Nat. Mater.*, 2010, **9**, 821.
23 M.-Y. Cheng, C.-M. Tsao, Y.-Z. Lai and Y.-J. Yang, *Sens. Actuators, A*, 2011, **166**, 226.
24 M. Shimojo, A. Namiki, M. Ishikawa, R. Makino and K. Mabuchi, *IEEE Sens. J.*, 2004, **4**, 589.
25 R. D. P. Wong, J. D. Posner and V. J. Santos, *Sens. Actuators, A*, 2012, **179**, 62.
26 D. J. Lipomi, M. Vosgueritchian, B. C.-K. Tee, S. L. Hellstrom, J. A. Lee, C. H. Fox and Z. Bao, *Nat. Nanotechnol.*, 2011, **6**, 788.
27 S. Yao and Y. Zhu, *Nanoscale*, 2014, **6**, 2345.
28 F. Xu and Y. Zhu, *Adv. Mater.*, 2012, **24**, 5117.
29 M. Kaltenbrunner, T. Sekitani, J. Reeder, T. Yokota, K. Kuribara, T. Tokuhara, M. Drack, R. Schwödiauer, I. Graz, S. B. Gogonea, S. Bauer and T. Someya, *Nature*, 2013, **499**, 458.
30 J. M. Engel, N. Chen, K. Ryu, S. Pandya, G. Tucker, Y. Yang and C. Liu, *Solid State Sensors, Actuators, and Microsystems Workshop*, Hilton Head, SC, 2006, p. 316.
31 C.-X. Liu and J.-W. Choi, *J. Micromech. Microeng.*, 2009, **19**, 085019.
32 T. Sekitani, Y. Noguchi, K. Hata, T. Fukushima, T. Aida and T. Someya, *Science*, 2008, **321**, 1468.